

Transcriptome analysis reveals cyclobutane pyrimidine dimers as a major source of UV-induced DNA breaks

George A Garinis¹, James R Mitchell¹,
Michael J Moorhouse², Katsuhiko Hanada¹,
Harm de Waard¹, Dimitri Vandeputte¹,
Judith Jans^{1,5}, Karl Brand¹, Marcel Smid³,
Peter J van der Spek², Jan HJ
Hoeijmakers¹, Roland Kanaar^{1,4}
and Gijsbertus TJ van der Horst^{1,*}

¹Department of Cell Biology and Genetics, Erasmus University Medical Center, Rotterdam, The Netherlands, ²Department of Bioinformatics, Erasmus University Medical Center, Rotterdam, The Netherlands, ³Department of Medical Oncology, Josephine Nefkens Institute, Erasmus University Medical Center, Rotterdam, The Netherlands and ⁴Department of Radiation Oncology, Erasmus University Medical Center, Rotterdam, The Netherlands

Photolyase transgenic mice have opened new avenues to improve our understanding of the cytotoxic effects of ultraviolet (UV) light on skin by providing a means to selectively remove either cyclobutane pyrimidine dimers (CPDs) or pyrimidine (6-4) pyrimidone photoproducts. Here, we have taken a genomics approach to delineate pathways through which CPDs might contribute to the harmful effects of UV exposure. We show that CPDs, rather than other DNA lesions or damaged macromolecules, comprise the principal mediator of the cellular transcriptional response to UV. The most prominent pathway induced by CPDs is that associated with DNA double-strand break (DSB) signalling and repair. Moreover, we show that CPDs provoke accumulation of γ -H2AX, P53bp1 and Rad51 foci as well as an increase in the amount of DSBs, which coincides with accumulation of cells in S phase. Thus, conversion of unrepaired CPD lesions into DNA breaks during DNA replication may comprise one of the principal instigators of UV-mediated cytotoxicity.

The EMBO Journal (2005) 24, 3952–3962. doi:10.1038/sj.emboj.7600849; Published online 27 October 2005

Subject Categories: genome stability & dynamics; genomic & computational biology

Keywords: DNA damage; functional genomics; photolyase; UV irradiation

*Corresponding author. Department of Cell Biology and Genetics, Center for Biomedical Genetics, Erasmus University Medical Center, PO Box 1738, 3000 DR Rotterdam, The Netherlands. Tel.: +31 10 408 7455; Fax: +31 10 408 9468; E-mail: g.vanderhorst@erasmusmc.nl

⁵Present address: Medical Genetic Center, Department of Molecular and Cell Biology, University of California at Berkeley, 125 Koshland Hall, Berkeley, CA, USA

Received: 9 June 2005; accepted: 30 September 2005; published online: 27 October 2005

Introduction

Ultraviolet (UV) radiation comprises one of the major exogenous toxic agents through which cellular macromolecules can be damaged, thereby inducing deleterious effects such as sunburn, immune suppression, skin cancer and photoaging (Friedberg *et al*, 1995). As nucleic acids, lipids and proteins are simultaneously damaged during UV exposure, it has been difficult to pinpoint the principal cellular target for the UV response. With respect to DNA, cyclobutane pyrimidine dimers (CPDs) and pyrimidine (6-4) pyrimidone photoproducts (6-4PPs) are the predominant lesions caused by short-wavelength UV radiation (Mitchell, 1988). Both types of lesions impinge on vital cellular functions, including transcription, DNA replication and cell cycle progression. Their persistence in the genetic material also increases the chance of fixation into mutations, a hallmark event of cancer initiation (Friedberg *et al*, 1995).

A number of mechanisms have evolved to recognize and remove DNA damage. For bulky helix-distorting damage, such as the main UV-induced lesions, the principal repair mechanism is the evolutionarily conserved nucleotide excision repair (NER) pathway (Hoeijmakers, 2001). Two different modes of lesion recognition delineate distinct NER subpathways. Transcription-coupled NER is restricted to repair of damage on the transcribed strand of active genes and is efficient at removing CPDs and 6-4PPs, in addition to other types of transcription-blocking lesions. Global genome NER (GG-NER) removes DNA damage from any position in the genome (Hoeijmakers, 2001). However, whereas 6-4PPs and other types of helix-distorting lesions are efficiently repaired, CPDs form a poor substrate and are removed at significantly reduced rates in human cells (Tung *et al*, 1996), and virtually not at all in rodent cells (Bohr *et al*, 1985). During DNA replication, cells can bypass persisting CPDs by employing relatively error-free or error-prone bypass polymerases, or by utilizing template switching, involving proteins of the homologous recombination repair pathway (Hoeijmakers, 2001). Failure of these pathways may lead to arrested replication forks, requiring subsequent processing for recombinational repair and thereby increasing the chance of chromosomal aberrations. Thus, based on their high relative abundance, slow repair kinetics and known mutagenicity, CPDs are thought to contribute significantly to the effects of UV radiation (Mitchell, 1988; Sage, 1993; Tung *et al*, 1996; Yoon *et al*, 2000). In humans, the essential role of NER in the repair of UV-induced cytotoxic photolesions is illustrated by the occurrence of photosensitive disorders (e.g. xeroderma pigmentosum) that originate from inborn errors in NER genes (Bootsma *et al*, 2002).

A distinct strategy to repair UV-induced photolesions is photoreactivation (PR), an enzymatic reaction in which 6-4PPs or CPD lesion-specific photolyases directly revert photolesions into undamaged bases using visible light energy (Carell *et al*, 2001). However, although photolyases are present across species boundaries, they are absent in placental mammals. We have previously established mice that express a

marsupial (*Potorous tridactylis*) CPD-specific photolyase transgene either ubiquitously or specifically in the basal keratinocytes of the epidermis. These mice were used to dissect the specific contributions of CPDs versus 6-4PPs to the biological consequences of UV irradiation (Chigancas *et al*, 2000; Schul *et al*, 2002). Importantly, light-dependent removal of CPDs but not 6-4PPs was found to promote UV survival (Chigancas *et al*, 2000; Schul *et al*, 2002; Nakajima *et al*, 2004). Moreover, CPDs appeared to be the primary cause of the vast majority of (semi) acute responses in the UV-exposed skin (i.e. sunburn, apoptosis, hyperplasia and mutation induction) and have been unequivocally identified as the principal instigator of non-melanoma skin cancer (Jans *et al*, 2005).

In the current study, we aimed at identifying those pathways through which unrepaired CPDs might induce their harmful effects. By implementing a functional genomics approach, we demonstrate that during DNA replication, unrepaired CPD lesions can be converted into a substantial source of toxic, replication-dependent single-strand breaks (SSBs) and double-strand breaks (DSBs), highlighting their role in UV-mediated cytotoxicity.

Results

Impact of CPDs on the transcriptional response to UV irradiation

To ascertain the global transcriptional response to UV damage in general and to CPDs specifically, CPD photolyase trans-

genic mouse dermal fibroblasts (MDFs) were irradiated with a series of UV doses (0, 2, 4 and 8 J/m²), treated with PR light or kept in the dark for 30 or 60 min and harvested at intervals from -30 min (relative to the 0 h time point that marked one full hour of PR light exposure) to +24 h (Figure 1A). Under the conditions used, we observed neither cell loss nor signs of apoptosis (i.e. TUNEL staining, ligation-mediated PCR amplification of fragmented DNA; data not shown). The effectiveness of CPD repair by photolyase was confirmed by immunocytochemical visualization of CPDs. As shown in Figure 1B, CPDs were no longer detectable after 1 h exposure to PR light. In contrast, when cells were kept in the dark (thus withholding the energy required for photolyase activity), CPDs remained visible, which is consistent with their poor removal by GG-NER in rodent cells (Bohr *et al*, 1985). Next, we determined the gene expression profiles by microarray analysis, using 15K cDNA arrays (see Materials and methods). To assess whether PR of UV-induced CPDs has a substantial impact on gene expression, we examined, by unsupervised hierarchical clustering, the similarity of transcription profiles of all responsive genes (defined as those genes for which the expression changed significantly in time and with UV dose; ANOVA *P*-value ≤ 0.05, ±1.5-fold change). As shown in Figure 2A, the profound effect of PR (and therefore CPD removal) on the transcriptional response to UV was readily seen at each of the time points examined after PR. For each time point, at a given UV dose, all matrix points clustered into two main groups correlating solely with

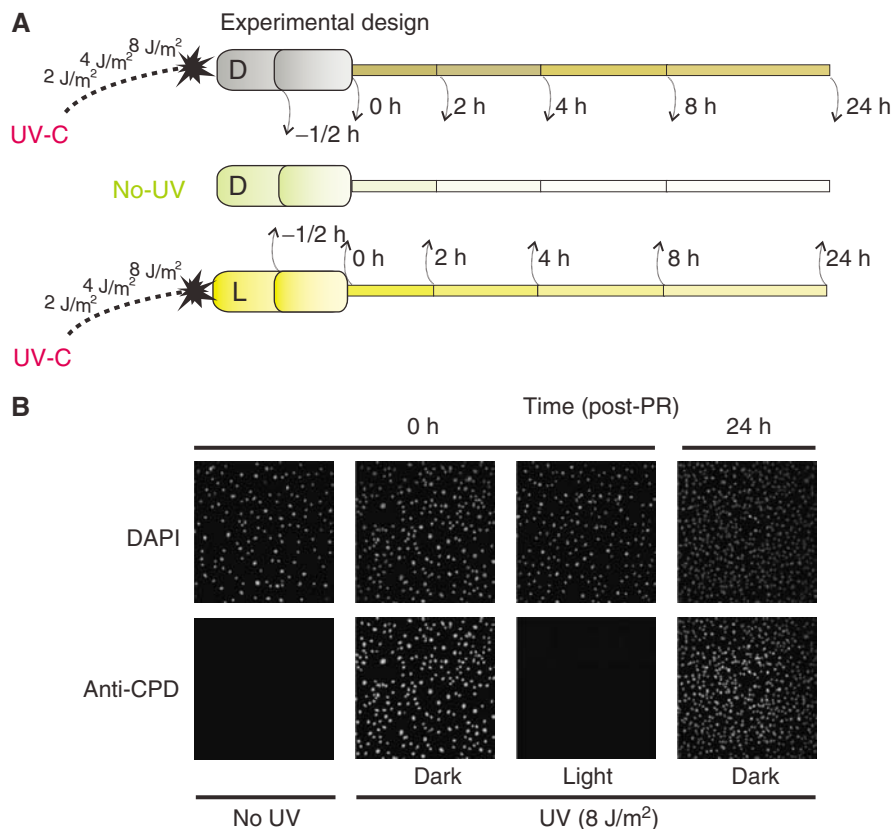


Figure 1 Experimental approach and removal of CPDs upon PR. (A) Graphical representation of the experimental design. For each dose and time point, labelled cDNAs derived from irradiated, PR and non-PR samples (upper and lower horizontal bars) were hybridized to unirradiated, non-PR material from the same time point (middle bar). D: dark; L: light. (B) CPDs were detected by indirect immunofluorescence; nuclei were visualized by DAPI staining. UV dose (No UV or 8 J/m²) and PR status (light or dark) are indicated on the bottom; time after the 1 h PR period is indicated on top.

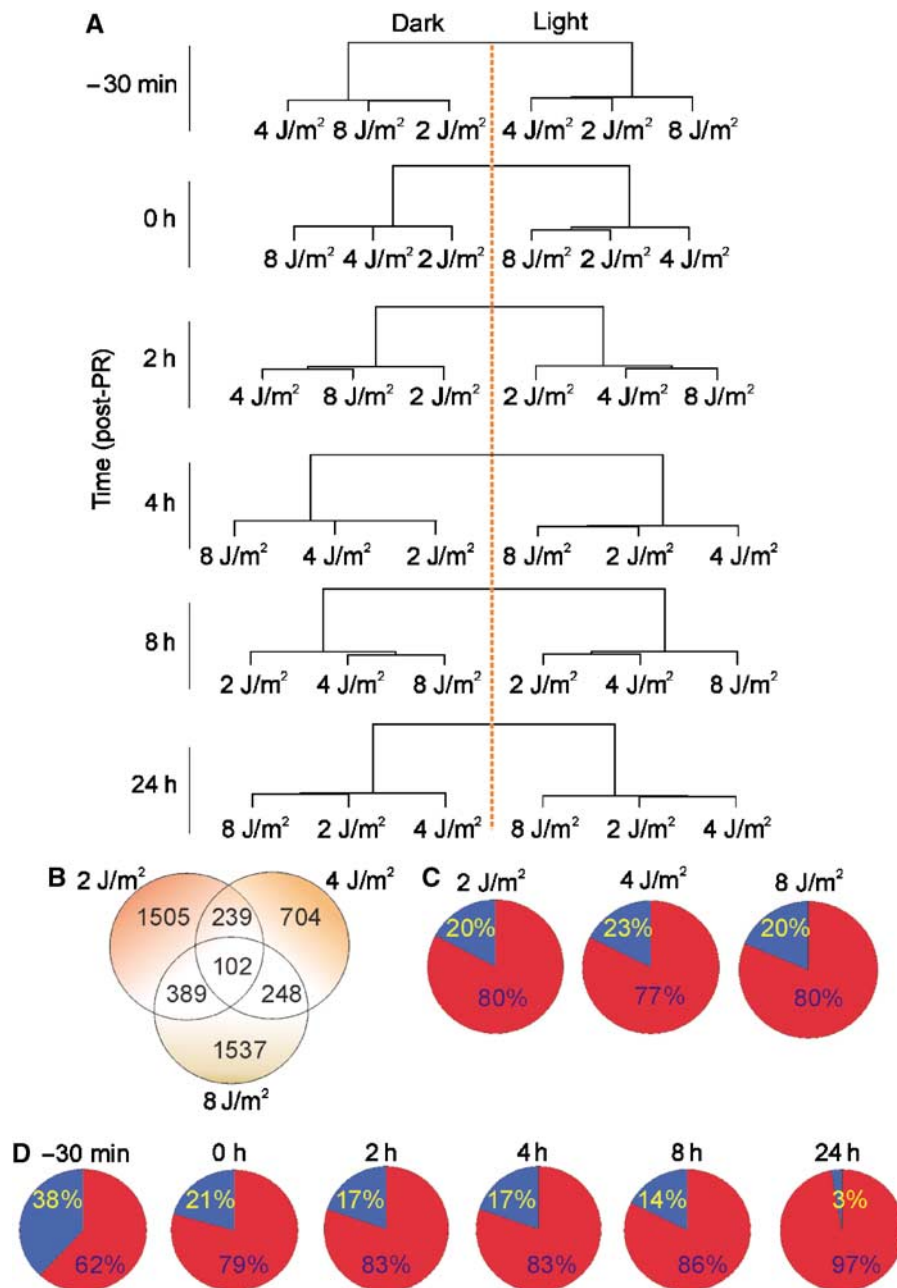


Figure 2 PR of CPDs is a major determinant of significant gene expression profiles. (A) Tree graph representation of the similarity between significant expression profiles (ANOVA $P \leq 0.05$, $\geq \pm 1.5$ -fold change) at a given time point. Note the clustering of all matrix points (defined as a unique combination of dose and time point) into two main groups correlating to dark or light exposure during PR (to the left and right of the dotted orange line, respectively). (B) Venn diagrams of 2, 4 and 8 J/m² biosets. Each bioset represents all significant genes in at least one time point (0–24 h) at the corresponding dose (2, 4 and 8 J/m²) in the absence of PR. (C) CPD-dependent and -independent gene expression. Each bioset from (B) was divided into blue, depicting the percentage of genes shared between both PR and non-PR MDFs (CPD-independent), and red, depicting the percentage of genes present only in the absence of PR (CPD-dependent). (D) Time dependence of the shared transcriptional response. The 8 J/m² bioset representing all significant genes at each individual time point (–30 min to 24 h) was divided proportionately into blue and red representing CPD-independent and -dependent gene expression, respectively.

their PR status, suggesting that light-dependent removal of CPDs was a major determinant of significant gene expression changes. This effect was further confirmed by an additional clustering over all 15 241 probes (Supplementary Figure S1A–F), thus avoiding any gene preselection or potential introduction of bias. These findings demonstrate the overriding influence of unrepaired CPDs on the genome-wide transcriptional shifts observed after UV exposure, validating the

biological effect of PR and our ability to measure it on a transcriptional level using this experimental approach.

Relative contribution of CPD lesions to the UV-induced transcriptional response

To delineate the relative contribution of CPDs to the overall transcriptional response to UV exposure in normal cells, we first created a series of ‘biosets’ composed of all genes

responding significantly to a given UV dose (2, 4 or 8 J/m² of UV-C) in any of the time points within 24 h after irradiation (Figure 2B). Then, we examined which of the genes in each of the three UV dose biosets obtained from non-PR cells (when CPDs were present) also varied significantly in the 24 h period following exposure of cells to PR light (when CPDs were below the level of detection). This allowed us to identify those genes whose expression levels were affected by UV exposure in a CPD-dependent manner (Figure 2C). At all doses tested, only ~20% of the UV-responsive genes were also regulated in UV-treated cells that were exposed to PR light (Figure 2C). Similarly, when we compared the distinct and shared significant transcriptional responses of PR and non-PR cells (exposed to 8 J/m²), we identified the highest percentage of shared genes (38%) to occur at the earliest time point (-30 min; Figure 2D). This percentage gradually declined to only 3% at the latest time point (24 h), suggesting that most non-CPD lesions (including 6-4PPs) are repaired within the 24 h period following UV, with the transcriptional response at the latest time point (24 h) reflecting the presence of persisting CPDs in the genome. Taken together, our data provide strong evidence that DNA lesions, rather than damaged proteins and/or lipids, are the principal mediators of the transcriptional response to UV exposure with CPDs representing the primary determinant.

Impact of CPD-dependent transcriptional responses on UV-induced biological processes

To identify the biological processes provoked by CPDs in UV-exposed cells, all responsive genes from each bioset were subjected to gene ontology (GO) classification and subsequent network analysis (Supplementary Figure S2; data available at http://www.eur.nl/fgg/ch1/gene_network). Those biological processes containing a significantly disproportionate number of responsive genes relative to those printed on the microarrays were red-flagged as over-represented. Upon 8 J/m² of UV-C and in the absence of PR, a broad range of biological processes were significantly over-represented including that of nucleic acid (GO:0006139), lipid (GO:0006629) and protein metabolism (GO:0009058), corroborating our previous findings that the majority of UV-responsive genes required the presence of CPDs. A smaller number of processes were identified at lower doses, indicating that, over the 24 h period examined, the biological effect exerted by UV was proportional to the dose range.

Contribution of CPD lesions to the transcriptional regulation of genes associated with SSB/DSB signalling and repair

How and why do CPDs—which contrast 6-4PPs in that they are poorly recognized and inefficiently repaired by GG-NER and yet are tolerated in cells—exert influence on such a broad range of physiological processes? To answer this, we examined in an unbiased way the most predominant molecular networks underlying the response to DNA damage itself by implementing the Ingenuity Molecular Network analysis approach (www.ingenuity.com). First, all genes encoding products functioning in common networks (pathways) were annotated, and subsequently the statistical significance of each network was listed (see ‘network analysis’ online). In combination with the previous analysis for the over-representation of biological processes, this method avoided any

arbitrary data preselection, or bias in interpretation of the initially identified significant expression profiles. Strikingly, for the 8 J/m² bioset, the most significant network identified within the GO-tree categorization ‘response to endogenous stimulus’ (identified as an over-represented biological process itself and including all modes of DNA repair and the response to DNA damage itself; see online visualizations) was associated with strand break repair pathways. Importantly, all genes encoding products that share a common role in the repair of DSBs via homologous recombination (*Rad51*, *Rad54*, *Xrcc3* and *Blm*) and non-homologous end joining (*Ku80*) were differentially expressed only upon the continuing presence of CPDs (Figure 3A). Similarly, a network of genes with an overlapping role in the response to DNA break (including *Mre11a*, *Rad50*, *Rad51* and *Parp-2*) was identified at lower doses as well (Figure 3A and online visualization). With the exception of *Rad50*, all other genes were significantly differentially transcribed in UV-irradiated, non-PR MDFs only (and thus as a consequence of the presence of CPDs).

The initial finding that CPDs could contribute substantially to the transcriptional regulation of genes associated with SSB and DSB repair prompted us to further examine those pathways involved in signalling of such DNA breaks. Noticeably, within the GO-tree categorization ‘physiological processes’, we identified the most significantly over-represented network in the 8 J/m² bioset to contain genes directly involved in the ATM signalling pathway that is centrally involved in the detection and signalling of SSBs and DSBs in mammalian cells (*Atm*, *Chk2*, *Hus1*, *c-Abl-1*, *Mdm2*, *Blm* and *Cdc25a*; Figure 3A and online visualization). With the exception of *Mdm2*, which has a prominent role outside the signalling of DNA breaks as well, changes in expression levels of each of these genes correlated significantly with the presence of unrepaired CPDs. The accuracy of the microarray data for the genes involved in the repair of DSBs as well as additional modes of DNA repair was validated for *Rev1L*, *Atm*, *Xpc* (various time points), *Msh6*, *Atrx*, *Rad54L*, *Rad51*, *Cdc25a*, *Blm*, *Xrcc1*, *Xrcc3*, *Hus1*, *Smug1*, *Abl-1*, *MutYH*, *Xpg*, *Rad6* and *Fen1* using quantitative real-time (QRT)-PCR (Figure 3C and D).

To examine the biological relevance of the transcriptional response to SSBs and DSBs in an intact organism, we exposed CPD photolyase transgenic mice to 1 minimal erythemal dose of UV-B, followed by treatment of part of the skin with PR light for 3 h. At 8 h after treatment, unexposed, UV-exposed/non-PR and UV-exposed/PR areas of the skin were used to prepare RNA for QRT-PCR analysis. Similar to the *in vitro* results, we noticed the transcriptional upregulation of *Rad54*, *Rad51*, *Xrcc1*, *Xrcc3*, *Cdc25a* and *Hus1* in the skin of UV-irradiated mice, which could be prevented by PR (Figure 3E). Interestingly however, *Atm* demonstrated opposite expression directions in UV-treated, non-PR mouse skin as compared to MDFs, which again was prevented by PR, suggesting a difference in the kinetics of the repair and signalling response with respect to time after UV-B irradiation.

CPD lesions trigger accumulation of γ -H2AX, P53bp1 and Rad51 foci

As UV-induced photolesions are known to obstruct replicative polymerases, we next investigated whether replication intermediates could account for the observed CPD-dependent

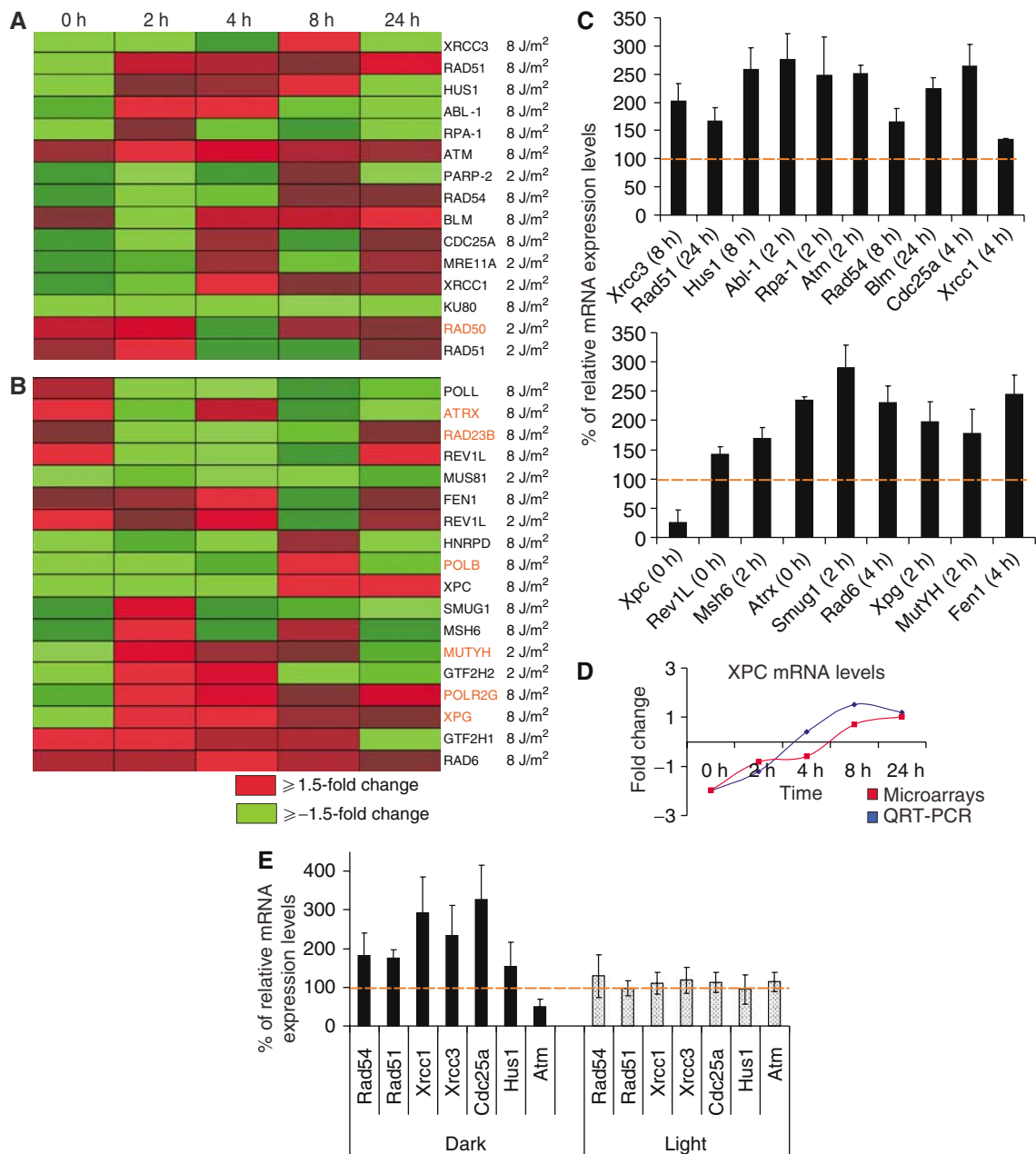


Figure 3 CPDs provoke the transcriptional response of genes associated with replication-dependent and -independent modes of DNA damage repair. **(A)** Heat map representation of time-dependent expression profiles of genes associated with SSB/DSB repair and signalling. **(B)** Additional modes of DNA repair in UV-irradiated, non-PR-treated MDFs as compared to non-UV, non-PR-treated MDFs. Changes in fold expression are represented by red (upregulated $\geq +1.5$ -fold change) and green (downregulated ≥ -1.5 -fold change) as indicated. All other colors represent intermediate fold changes. Gene entries in orange represent those genes that displayed significant expression profiles upon removal of CPDs by PR. The 0 h time point includes the 1 h exposure to PR. **(C)** QRT-PCR verification of microarray data. Fold changes are expressed as percentage of relative mRNA expression for each gene in UV-irradiated (8 J/m² of UV-C), non-PR-treated MDFs as compared to non-irradiated, non-PR-treated MDFs at the indicated time points. **(D)** Time-dependent mRNA expression levels of XPC obtained from microarrays and real-time PCR as indicated in UV-irradiated, non-PR-treated MDFs as compared to non-irradiated, non-PR-treated MDFs. Fold changes are expressed in log₂ ratios. **(E)** QRT-PCR evaluation of genes associated with DSB repair and signalling in UV-irradiated, non-PR-treated mouse skin. Fold changes are expressed as percentage of the relative mRNA expression levels for each gene in the UV-irradiated, PR-treated mouse skin over the non-UV, non-PR-treated mouse skin 5 h after UV irradiation and subsequent PR treatment (3 h).

transcriptional response. Stalling of replication forks (as well as SSBs and DSBs produced by a variety of agents) can be visualized by the appearance of phosphorylated histone H2AX (γ -H2AX)-containing foci that accumulate at sites of DNA breaks (Fernandez-Capetillo *et al*, 2004; Squires *et al*, 2004; Ward *et al*, 2004; Halicka *et al*, 2005). In ~10% of the

untreated MDFs, we observed 1–2 γ -H2AX foci per nucleus (Figure 4A), which likely reflects unrepaired, spontaneous DNA damage. In marked contrast, γ -H2AX staining of UV-irradiated, non-PR MDFs revealed a punctuate pattern of foci that gradually accumulated from 1–2 foci/nucleus 2 h after UV irradiation (~20% positive cells) to approximately 17

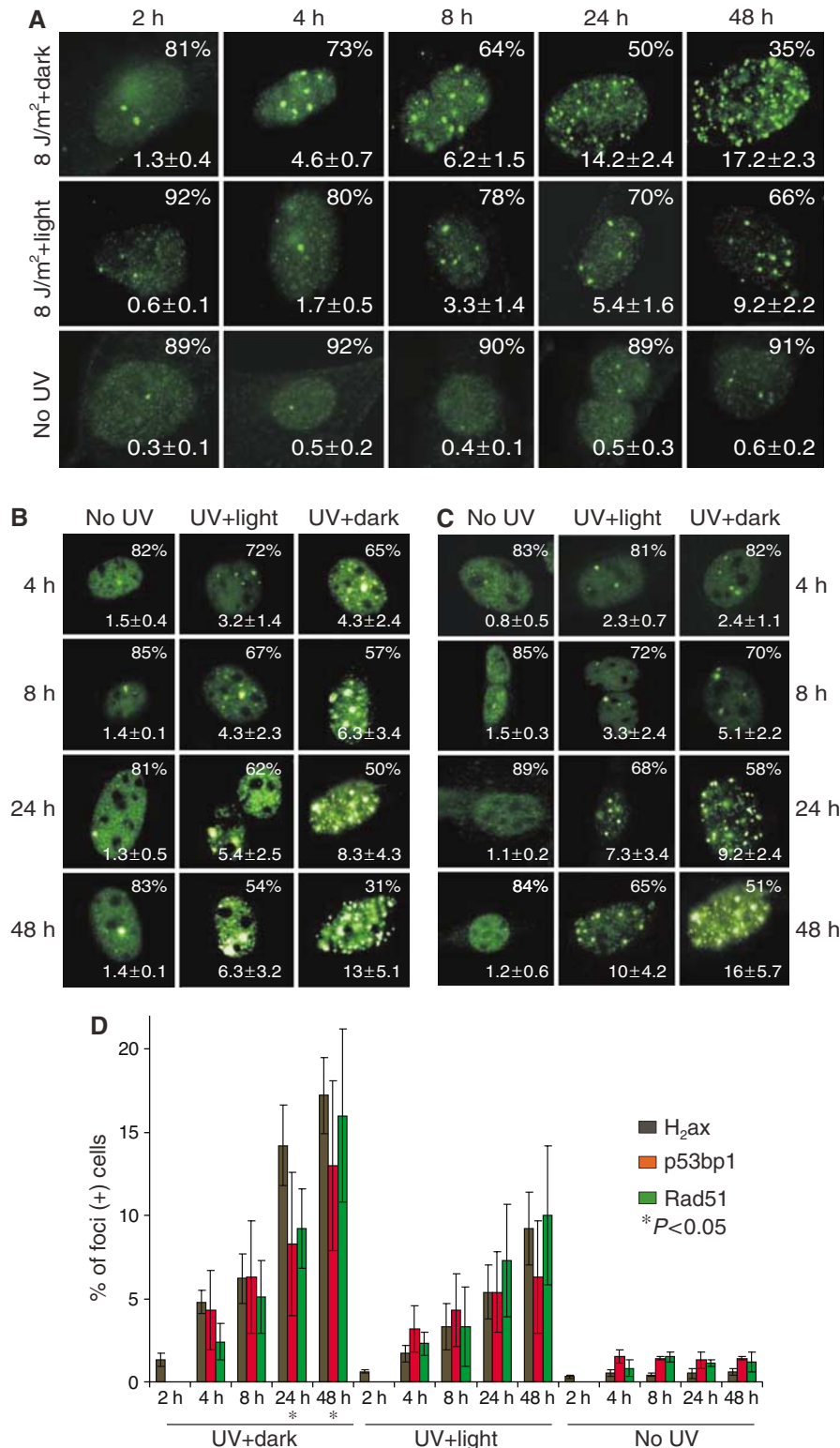


Figure 4 CPDs induce accumulation of γ -H2AX, P53bp1 and Rad51 foci. (A) MDFs stained with anti- γ -H2AX at 2, 4, 8, 24 and 48 h after UV exposure and subsequent PR (or not). Upper, middle and lower panels: UV-exposed, non-PR-treated (UV + dark), PR-treated (UV + light) and unirradiated (No UV) MDF cultures. (B) MDFs stained with anti-P53bp1 at 4, 8, 24 and 48 h after UV exposure and subsequent PR (or not). Left, middle and right panels: Unirradiated (No UV), UV-irradiated, PR-treated (UV + light) and non-PR-treated (UV + dark) MDF cultures. (C) MDFs stained with anti-Rad51 at 4, 8, 24 and 48 h after UV irradiation and subsequent PR (or not). Left, middle and right panels: Unirradiated (No UV), UV-irradiated, PR-treated (UV + light) and non-PR-treated (UV + dark) MDF cultures. Each image represents a projection of all optical sections through a typical cell. The number of foci per cell (average \pm standard deviation) representing only those fluorescent spots with an area larger than $0.24 \mu\text{m}^2$ (see Materials and methods) and the percentage of foci-free cells are shown in the lower and upper right corners, respectively. (D) Number of γ -H2AX, P53bp1 and Rad51 foci per cell in UV-irradiated, non-PR-treated (UV + dark), PR-treated (UV + light) and unirradiated (No UV) MDFs at the indicated time points.

foci/nucleus at 48 h after UV exposure (~65% positive cells; Figure 4A, 8 J/m² + dark). Removal of CPD lesions by PR substantially decreased the incidence of γ -H2AX foci to approximately 9 foci/nucleus (34% positive cells) at 48 h after treatment. Therefore, UV-induced γ -H2AX foci formation depends on the presence of persisting CPDs (Figure 4A and D). To further substantiate this finding, we examined the ability of P53bp1 and Rad51 to form foci upon UV irradiation. P53bp1 responds to ionizing radiation-induced DSBs by relocating to discrete nuclear foci, along with Mre11-Nbs-Rad50 complex and phosphorylated γ -H2AX (Schultz *et al*, 2000; Anderson *et al*, 2001; Rappold *et al*, 2001). Rad51 promotes DNA strand exchange on the processed single-stranded ends of the broken DNA during repair of DSBs by homologous recombination and can also be visualized as foci (Elliott and Jasin, 2002). In line with the accumulation of γ -H2AX foci, P53bp1 and Rad51 foci accumulated from 3–4 foci/nucleus to approximately 13 and 16 foci/nucleus, respectively, at 48 h after UV exposure (69 and 49% positive cells, respectively; Figure 4B and C). Importantly, PR-mediated removal of CPDs reduced significantly the incidence of P53bp1 and Rad51 foci to approximately 6 and 10 foci/nucleus, respectively (Figure 4B–D), indicating that the UV-induced formation of both P53bp1 and Rad51 foci requires the continuing presence of CPDs in the genome.

Detection of DSBs in the presence of CPDs

In addition to marking DSBs or potentially collapsed replication forks, γ -H2AX foci also form upon NER- and ATR-dependent processing of UV-induced photolesions (O'Driscoll *et al*, 2003), a process involving breaks in only one DNA strand. In order to distinguish CPD-induced DSBs from DNA excision repair intermediates, we analyzed genomic DNA from UV-treated PR and non-PR cells by pulsed-field electrophoresis (Figure 5A). In the absence of PR, we detected increased amounts of low-molecular-weight DNA, indicative of the presence of DSBs beginning at 16 h after UV irradiation (Figure 5A, irradiated cells, lanes marked –). Importantly, in line with the immunocytochemical results, DSB levels remained at background level upon complete removal of CPDs (Figure 5A, irradiated cells, lanes marked +). Under these experimental conditions, MDFs were refractory to apoptosis or necrosis. It is therefore unlikely that the CPD-dependent DSBs result from DNA fragmentation; rather they represent replication-dependent DNA breaks.

CPD-induced DSBs interfere with cell cycle progression

We next sought evidence for the DNA replication dependence of the observed CPD-induced DSBs by examining the impact of CPDs on cell cycle progression of UV-irradiated MDFs (8 J/m²) exposed to PR light or kept in the dark, using BrdU labelling and subsequent fluorescent activated cell sorting (FACS) sorting. As shown in Figure 5B, UV-exposed cells continued to incorporate BrdU for up to 8 h regardless of PR, but at a substantially lower level than unirradiated cells, an observation that is consistent with a slowing down of DNA replication. After 16 h however, PR cells incorporated BrdU as efficiently as unirradiated cells, thus indicating a return to normal cell cycling after an initial replication delay. In contrast, non-PR cells largely stopped incorporating BrdU altogether, suggesting that persisting CPD lesions cause a DNA replication catastrophe. Importantly, the moment of S-phase

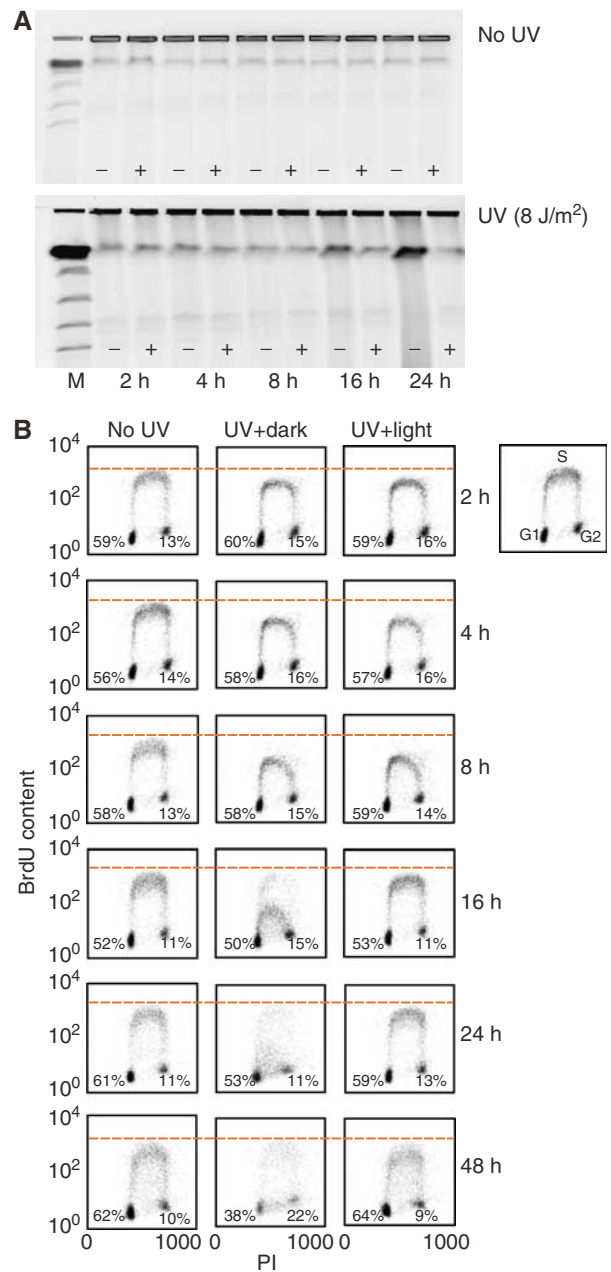


Figure 5 CPDs induce the accumulation of DSBs and an S-phase cell cycle arrest. (A) Detection of DSBs by pulsed-field electrophoresis in genomic DNA isolated from unirradiated (No UV) and UV-irradiated MDFs (UV) exposed to PR light (+) or not (–). (B) FACS analysis of the cell cycle of irradiated MDFs in the presence or absence of CPDs. The DNA (stained with propidium iodide, PI) and BrdU content of the cells is shown on the x- and y-axis, respectively. The left, middle and right panels show the effect of non-irradiated (No UV), irradiated/non-PR-treated (8 J/m² + dark) and irradiated/PR-treated (8 J/m² + light) cells, respectively, from 2 to 48 h subsequent to 8 J/m² of UV exposure and PR. The dotted line indicates the BrdU content of non-irradiated (left panel) versus that of irradiated cells in the absence (middle panel) or presence (right panel) of PR. Percentage of cells in G1 and G2 phases of the cell cycle is indicated.

cell cycle arrest coincided with the time point at which DSBs were clearly detected (16 h post-UV), which strongly implicates an S-phase DNA replication dependency of DSB formation. From these data, we conclude that the initial slowing

down of cell cycle progression (up to 8 h post-UV) was independent of persisting CPDs (likely due to combined *cis* and *trans* effects from the initial presence of CPDs, 6-4PPs and non-DNA-based lesions), whereas S-phase arrest was CPD-dependent and coincided with DSBs, which further points to DSBs as the consequence of collapsed replication forks or intermediates in their repair.

CPD-mediated transcriptional response of genes associated with additional modes of DNA repair

Consistent with the replication-dependent secondary effects of CPDs, we observed a significant upregulation of the expression of genes involved in error-free post-replication repair (PPR) (*Rad6A*, 4 h/8 J/m²) and error-prone PPR (*Rev1L*, 0 h at both low and high UV doses) (Figure 3B). Furthermore, our analysis revealed a CPD-dependent and -independent upregulation of two mismatch repair genes (*Msh6* at 2 h/8 J/m² and *MutY* at 2 h/2 J/m²).

Replication-independent modes of DNA repair, including NER and base excision repair (BER) pathways, also appeared transcriptionally regulated in cells exposed to 8 J/m² UV-C. After an initial decrease in the steady-state transcript levels at early time points, expression of the *Xpc* (Figure 3B–D) and *Rad23B* (Figure 3B) genes, encoding two initiators of GG-NER, is upregulated. Unlike *Xpc*, *Rad23B* expression was independent of persisting CPDs. In addition, the endonuclease *Xpg* (2 h/8 J/m²), two components of the DNA repair/transcription initiation complex TFIIH (*p44*, 2 h/2 J/m² and *p62* 2 h at both 2 and 8 J/m²) as well as *Polβ* (8 h/8 J/m²) and *Smug1* (2 h/8 J/m²), typically associated with BER and/or repair of SSBs, were transcriptionally regulated, with *Polβ* displaying a CPD-independent regulation (Figure 3B). Finally, in cells exposed to 8 J/m² UV-C, we observed the early transcriptional upregulation of ATR-X, a type II helicase with homology to Rad54 that has been previously implicated in NER and transcription (Stayton *et al*, 1994).

Stochastic cis-acting effects of UV on global gene transcription

It has long been hypothesized that expression of genes with relatively longer primary transcript lengths may be at greater risk to transcription-blocking lesions than shorter ones. Within the first 4 h following PR, we observed a significant correlation between transcript length, increased number of genes with a negative fold change and decreased number of genes with a positive fold change at both 2 and 8 J/m² data sets (Supplementary Figure S3, solid bars, shown at 0 h after PR). Importantly, this effect was lost upon removal of CPD lesions following PR, with the difference between up- and downregulated genes being equally pronounced regardless of their length (Supplementary Figure S3, open bars). Thus, a stochastic *cis*-acting steric hindrance induced by CPDs may comprise a substantial threat to the timely, coordinated transcriptional response to immediate threats (i.e. exogenous DNA-damaging agents).

Discussion

We have previously shown that complete removal of CPDs by PR *in vivo* prevents the onset of acute effects (apoptosis, epidermal hyperplasia and erythema) and long-term res-

ponses (non-melanoma skin cancer) in the UV-exposed skin of CPD photolyase transgenic mice (Jans *et al*, 2005). To gain insight into the transcriptional response elicited by CPDs, we employed a functional genomic approach on UV-exposed isogenic murine cells expressing a CPD photolyase transgene that allows rapid removal of CPD lesions in a light-dependent manner.

CPDs have a profound effect on the transcriptional response to UV irradiation

As could be predicted on the basis of the pronounced attenuation of (semi)-acute effects in UV-exposed cells and skin through PR of CPD lesions, we have found that photolyase-mediated removal of CPDs has a considerable impact on gene expression profiles in our model cellular system. The fact that all matrix points clustered into two main groups correlating with the PR status of the UV-exposed cell (Figure 2A) confirmed the effect of PR on the transcriptional response to UV and validates our experimental approach to detect transcriptional changes.

Besides DNA, other UV wavelength-absorbing cellular macromolecules such as RNA (Iordanov *et al*, 1997, 1998) and proteins (Coffer *et al*, 1995) have been put forward as primary instigators of the response to UV exposure. Furthermore, radiation-induced effects can also be observed in unirradiated cells via the bystander effect (Goldberg and Lehnert, 2002). As the light-dependent removal of CPDs negated ~80% of the observed transcriptional response (Figure 2C) and the affinity of CPD photolyase for CPD dimers in rRNA is considerably less than in DNA ($K_a = 10^2$ in rRNA versus 10^8 in DNA) (Yasui and Eker, 1998), our data provide evidence that damaged DNA (rather than RNA) is the principal mediator of the cellular transcriptional response to UV with CPDs as the primary (if indirect) stimulus. As the initial CPD damage load is rapidly declining during the 1 h PR period, our data indicate that the remaining ~20% of UV-responsive genes shared by PR and non-PR UV-exposed cells represent the transcriptional response to non-CPD DNA lesions such as 6-4PPs, thymine glycols and protein–DNA crosslinks, as well as a variety of other damaged cellular macromolecules, including proteins and lipids.

CPDs induce the transcriptional regulation of genes associated with repair and signalling of SSBs and DSBs

It remained elusive, however, why the removal of CPDs (which are poorly recognized by the GG-NER system) negated most of the (semi) acute responses *in vivo* (Schul *et al*, 2002; Jans *et al*, 2005) as well as the observed effects on the transcriptional response (both in terms of number of genes and categories of different responses) to UV *in vitro* (Figure 2C and D; a detailed overview is available online). We have tackled this question by employing an unbiased approach (instead of an arbitrary gene preselection) that combined network analysis, GO categorization and analysis of significantly over-represented biological processes. This led us to identify (i) the nature of the DNA damage itself, (ii) the signalling mechanisms involved and (iii) the implicated biological processes.

This approach revealed several genes implicated in the repair of DNA breaks (*Rad51*, *Rad54*, *XRCC3*, *Blm*, *KU80*, *Mre11a* and *Parp-2*) to respond to the continuous presence of CPDs in the genome (Figure 3A). Thus, DNA replication forks

blocked by CPDs may eventually collapse, giving rise to single-strand intermediates and eventually DSBs, or else may require processing that involves formation of transient DSBs. In either case, homologous recombination will be employed to repair the collapsed fork (Cox *et al*, 2000).

In mammalian cells, however, a successful response to DNA damage is heavily dependent on their ability to activate a series of signalling events that will delay cell cycle progression until optimal repair can be achieved. Having identified persistent CPDs in the genome as the likely trigger for the induction of a combination of repair intermediates including stalled replication forks, SSBs and/or DSBs, we examined whether pathways relevant to the detection and signalling of these highly toxic lesions were regulated as well. Strikingly, among the most significantly over-represented networks detected in this microarray study, was the ATM signalling pathway (Figure 3A and online visualization), centrally involved in the detection and signalling of DSBs in mammalian cells (Kurz and Lees-Miller, 2004). In MDFs, this pathway displayed a noticeable specificity to CPDs (Figure 3A and online visualization), which was confirmed by QRT-PCR at the corresponding time points. The *in vivo* relevance of this finding was confirmed in UV-irradiated, PR and non-PR mouse skin. Taken together, these data suggest that in rapidly dividing cells, such as the basal keratinocytes, UV-induced photolesions (i.e. CPDs) with the potential to block replication cause subsequent damage when encountered by a replication fork, including SSBs and DSBs. These toxic intermediates, rather than CPDs themselves, are therefore most likely to be the signals responsible for the triggering of the above gene networks.

Unrepaired CPD lesions induce DSBs and S-phase cell cycle arrest

γ -H2AX, P53bp1 and Rad51 foci form rapidly following ionizing irradiation (Schultz *et al*, 2000; Elliott and Jasin, 2002; Fernandez-Capetillo *et al*, 2004; Squires *et al*, 2004; Ward *et al*, 2004; Halicka *et al*, 2005) and are thought to mark the presence of genomic DSBs. Although it is known that UV irradiation can lead to replication-dependent γ -H2AX foci formation and DSBs (Squires *et al*, 2004; Ward *et al*, 2004; Halicka *et al*, 2005), this toxic intermediate is still not commonly associated with the normal spectrum of UV-induced DNA lesions. The present study unequivocally shows that γ -H2AX, P53bp1 and Rad51 foci accumulated gradually in the presence of persisting CPDs. The number of γ -H2AX foci did not substantially increase until 8 h after exposure to UV irradiation in non-PR cells and required an additional 16 h to accumulate in 50% of the cells (Figure 4A). Similarly, the number of P53bp1 and Rad51 foci did not accumulate significantly until 24 h, whereas in the case of Rad51, it required an additional 24 h to accumulate in 50% of cells (Figure 4B and C). Thus, CPD-mediated γ -H2AX, P53bp1 and Rad51 foci formation clearly differs from γ -irradiation-mediated foci formation. For example, foci of γ -H2AX are known to appear in all cells within minutes after irradiation (Rogakou *et al*, 1999). Importantly, the detection of DSBs indicates that CPD-dependent formation of γ -H2AX, P53bp1 and Rad51 foci proceeds through formation of DSBs (Figure 5A).

The kinetics of CPD-induced γ -H2AX, P53bp1 and Rad51 foci formation upon UV treatment, and the coincidence with

DSB formation suggest cell cycle dependency. Primary human fibroblasts do not respond to DSBs by arresting cell cycle progression until they reach S phase (Kaufmann and Kies, 1998). UV-irradiated non-PR MDFs accumulated gradually in S phase (Figure 5B). The onset of S-phase arrest (16 h) coincided with the time frame in which DSBs were detected by pulsed-field gel electrophoresis, suggesting that the S phase of the cell cycle is critical for DSB formation, probably in response to stalled replication forks. However, in the presence of CPDs, the fraction of cells arrested in S phase 48 h after UV exposure was substantially less than the fraction of γ -H2AX, P53bp1 and Rad51 foci positive cells within the same time period, which suggests that foci may not only signal the formation of DSBs but also the appearance of stalled replication forks and SSBs.

CPDs exert pleiotropic effects via both replication-dependent and replication-independent repair intermediates

Whatever its origin, replicative blockage needs to be repaired or bypassed to resume the process of replication. In mammals, mutagenic bypass of DNA damage is equivalent to error-prone translesion replication (Pages and Fuchs, 2002), a process that requires the RAD6A protein (Barbour and Xiao, 2003). Here, we observed a CPD-dependent upregulation of *Rad6A* gene expression 4 h after cells have been exposed to 8 J/m² UV-C (Figure 3B). Error-free and error-prone modes of PPR differ, based on the polymerase employed to bypass the lesion. We also observed that UV exposure (2 and 8 J/m²) elicits an immediate (0 h time point) upregulation of *Rev1L* expression. Inhibition of error-prone bypass by disruption of the polymerase zeta-associated *Rev1L* gene product greatly reduces the UV-induced mutation frequency without affecting cell survival (Gibbs *et al*, 2000). Thus, upregulation of *Rad6A* and *Rev1L*, although important for prevention of replication blocks, is likely to contribute to mutation induction after UV exposure. Lesion bypass, especially by error-prone polymerases, can lead to mismatches in nascent DNA opposite the photolesion and mismatch repair proteins have been implicated in the repair of such damage (Wang *et al*, 1999). The significant upregulation of both *Msh6* and *MutY* genes suggests that UV-exposed DNA may directly signal the presence of CPD lesions in the genome, a strategy that is anticipated to avoid mutation fixation by replication or excision repair.

Although most of the NER genes are thought to be ubiquitously expressed in mammalian cells, the *Xpc* and *p48* genes (encoding GG-NER-specific proteins) have been shown to be transcriptionally induced upon UV in a p53-dependent, replication-independent manner (Hwang *et al*, 1999; Adimoolam and Ford, 2002). Here, upon exposure to 8 J/m² UV-C, we observed coordinate transcriptional regulation of *Xpc* and *Rad23b* encoding the binding partner of the XPC protein (Ng *et al*, 2003; Figure 3B and D). Unlike *Xpc*, *Rad23B* expression was independent of persisting CPDs, suggesting its involvement in a wider range of stress-induced activities than NER alone. Interestingly, the initial decrease in *Xpc* mRNA levels (Figure 3D) was previously documented in normal human fibroblasts and adenocarcinoma cells (Adimoolam and Ford, 2002). Although the *Xpc* gene spans a relatively large region (~30 kb), a UV-induced *cis*-mediated transcription-blocking effect cannot fully explain the underlying cause of the early decrease in *Xpc* mRNA levels, as a

variety of genes with similar or larger primary transcript lengths failed to demonstrate comparable expression profiles. Other transcriptionally regulated NER components include the endonuclease *Xpg* and two components of the DNA repair/transcription initiation complex TFIIH (*p44* and *p62*) involved in unwinding DNA surrounding a lesion. Components involved in BER and/or repair of SSBs such as *Polβ* and *Smug1* were regulated at the level of gene transcription, although *Polβ* did not require the presence of CPDs in the genome.

CPDs induce cis-acting effects on global gene expression

Finally, our results show that gene-length-dependent transcriptional interference (Supplementary Figure S3), long predicted but never visualized on a global level in mammalian cells, is likely to be one source of selective pressure against long intron size in genes required for immediate response to genotoxic insult, as has been shown previously for genes required at high constitutive levels (Castillo-Davis *et al*, 2002) and for genes that are transcriptionally activated by the stress-induced tumor suppressor p53 (McKay *et al*, 2004).

Concluding remarks

Using photolyase-transgenic mouse cells that specifically remove UV-induced CPDs upon visible light exposure, we found that the presence of unrepaired CPD lesions (i) represents the principal mediator of the transcriptional response to UV (ii) induces the transcriptional regulation of genes associated with SSB and DSB signalling and repair, (iii) provokes the time-dependent accumulation of γ -H2AX, P53bp1 and Rad51 foci and (iv) increases the amount of DSBs coincident with an accumulation of cells in S phase. The relative abundance of CPDs over 6-4PPs (3:1 ratio) and the ability of NER-proficient cells to remove 6-4PPs faster than CPDs raises the question of whether a comparable amount of unrepaired 6-4PPs can elicit a response similar to the one described in this study. The answer to this question should come from studies with cells from totally NER-deficient (*Xpa*^{-/-}) CPD-PL and 6-4PP-PL (double) transgenic mice, in which the UV dose can be adapted to generate cells with equal amounts of unrepaired CPDs or 6-4PPs.

Taken together, our findings provide evidence that among UV-absorbing cellular macromolecules, DNA plays the most prominent role in downstream signalling of the damage response, implicating CPD-dependent replication products, rather than CPDs themselves, as the primary mediators of the bulk transcriptional response to UV light. The fact that the vast majority of (semi) acute and long-term responses in the UV-exposed skin (i.e. sunburn, apoptosis, hyperplasia, cancer initiation) have been previously ascribed to the continuing presence of CPDs in the genome raises the possibility for a direct role of replication-dependent SSBs and DSBs in UV-mediated cytotoxicity. Importantly, by identifying the nature of UV-induced SSBs and DSBs, our findings may pave the way for specific, downstream intervention strategies.

Materials and methods

Cell cultures, mouse skin samples, UV irradiation and PR

Culturing of MDFs, UV irradiation and PR were performed as described previously (Schul *et al*, 2002). Cells were UV-treated and

PR-treated (or not) for 30 or 60 min and harvested at the indicated time point. Mouse skin samples were obtained from the unexposed or irradiated skin area exposed to PR light (or not), as described previously (Jans *et al*, 2005).

Labelling and hybridization protocols

Labelling and hybridization protocols were adapted from the National Institute of Aging (NIA, Bethesda, MD). Samples were hybridized to unirradiated, non-PR MDFs of the pertinent time point. 15K cDNA microarrays were obtained from the Netherlands Cancer Institute. Detailed information on experimental design, total RNA isolation, cDNA labelling, hybridization and data extraction can be found in Supplementary data and at <http://microarrays.nki.nl/download/index.html>.

Data analysis

Hierarchical and K clustering, self-organizing maps and analysis of variance were performed by the Spotfire Decision Site software package 7.2 version 10.0 (Spotfire Inc., MA, USA). Detailed information on data processing, transcript retrieval and data analysis, GO classification and network analysis can be found at http://www.eur.nl/fgg/ch1/gene_network.

Immunofluorescence

CPDs, γ -H2AX and Rad51 were visualized by indirect immunofluorescence as previously described in irradiated (or not) cells that were subjected to PR (or not) and harvested for the indicated time points (Schul *et al*, 2002; Niedernhofer *et al*, 2004; van Veelen *et al*, 2005). P53bp1 foci were visualized with a rabbit polyclonal antibody to P53bp1 (Novus Biologicals, CO, USA). To assess, on a semiquantitative basis, the extent of foci formation, we considered only those foci with an area larger than 0.24 μm^2 . This conservative cutoff eliminates the contribution of nonspecific fluorescent spots in the background and actually results in an underestimate of the number of legitimate foci.

Pulsed-field gel electrophoresis

Subconfluent MDF cultures were exposed to 8 J/m² of UV-C, treated with PR (or not) and harvested for the pertinent time points. DSBs were detected by pulsed-field gel electrophoresis as described (Niedernhofer *et al*, 2004).

Flow cytometry and BrdU incorporation

Subconfluent MDF cultures were exposed to 8 J/m² of UV-C, treated with PR (or not), washed and grown for 2–48 h. At 1 h before each of the indicated time points, MDFs were incubated with BrdU (15 $\mu\text{g}/\text{ml}$), then harvested by trypsinization, fixed in 70% ethanol and stained with propidium iodide and α -BrdU antibody (1:1000; DAKO). The DNA content of the cells was determined by FACS sorting (FacsScan, Becton Dickinson). The percentage of cells in G1, S and G2 phases was calculated with CellQuest.

QRT-PCR

QRT-PCR was performed with the DNA engine Opticon (MJ Research, USA). For primer sequences and data analysis, see Supplementary data.

Data retrieval

Microarray data complied with the Minimum Information for Microarray Experiments (MIAME), submitted to European Bioinformatics Institute (EBI, Hinxton) and can be retrieved at <http://www.ebi.ac.uk/miamexpress> (Array: A-MEXP-76, Experiment: E-MEXP-117).

Supplementary data

Supplementary data are available at *The EMBO Journal* Online.

Acknowledgements

This work was supported by the Dutch Cancer Foundation (EUR 98-1774, EUR 2001-2437, EMCR 2002-2701), the Erasmus MC Revolving Fund (01-432), the Association for International Cancer Research (AICR 98-259, AICR 03-128) and the European Commission. JRM was a fellow of the Damon Runyon Cancer Research Fund (DRG 1677).

References

- Adimoolam S, Ford JM (2002) p53 and DNA damage-inducible expression of the xeroderma pigmentosum group C gene. *Proc Natl Acad Sci USA* **99**: 12985–12990
- Anderson L, Henderson C, Adachi Y (2001) Phosphorylation and rapid relocalization of 53BP1 to nuclear foci upon DNA damage. *Mol Cell Biol* **21**: 1719–1729
- Barbour L, Xiao W (2003) Regulation of alternative replication bypass pathways at stalled replication forks and its effects on genome stability: a yeast model. *Mutat Res* **532**: 137–155
- Bohr VA, Smith CA, Okumoto DS, Hanawalt PC (1985) DNA repair in an active gene: removal of pyrimidine dimers from the DHFR gene of CHO cells is much more efficient than in the genome overall. *Cell* **40**: 359–369
- Bootsma D, Kraemer KH, Cleaver JE, Hoeijmakers JH (2002) Nucleotide excision repair syndromes: xeroderma pigmentosum, Cockayne syndrome, and trichothiodystrophy. In *The Genetic Basis of Human Cancer*, Vogelstein B, Kinzler KW (eds) pp 211–237. New York: McGraw-Hill Medical Publishing Division
- Carell T, Burgdorf LT, Kundu LM, Cichon M (2001) The mechanism of action of DNA photolyases. *Curr Opin Chem Biol* **5**: 491–498
- Castillo-Davis CI, Mekhedov SL, Hartl DL, Koonin EV, Kondrashov FA (2002) Selection for short introns in highly expressed genes. *Nat Genet* **31**: 415–418
- Chigancas V, Miyaji EN, Muotri AR, de Fatima Jacysyn J, Amarante-Mendes GP, Yasui A, Menck CF (2000) Photorepair prevents ultraviolet-induced apoptosis in human cells expressing the marsupial photolyase gene. *Cancer Res* **60**: 2458–2463
- Coffer PJ, Burgering BM, Peppelenbosch MP, Bos JL, Kruijer W (1995) UV activation of receptor tyrosine kinase activity. *Oncogene* **11**: 561–569
- Cox MM, Goodman MF, Kreuzer KN, Sherratt DJ, Sandler SJ, Marians KJ (2000) The importance of repairing stalled replication forks. *Nature* **404**: 37–41
- Elliott B, Jasin M (2002) Double-strand breaks and translocations in cancer. *Cell Mol Life Sci* **59**: 373–385
- Fernandez-Capetillo O, Lee A, Nussenzweig M, Nussenzweig A (2004) H2AX: the histone guardian of the genome. *DNA Repair (Amst)* **3**: 959–967
- Friedberg EC, Walker GC, Siede W (1995) *DNA Repair and Mutagenesis*. San Francisco: WH Freeman and Company
- Gibbs PE, Wang XD, Li Z, McManus TP, McGregor WG, Lawrence CW, Maher VM (2000) The function of the human homolog of *Saccharomyces cerevisiae* REV1 is required for mutagenesis induced by UV light. *Proc Natl Acad Sci USA* **97**: 4186–4191
- Goldberg Z, Lehnert BE (2002) Radiation-induced effects in unirradiated cells: a review and implications in cancer. *Int J Oncol* **21**: 337–349
- Halicka HD, Huang X, Traganos F, King MA, Dai W, Darzynkiewicz Z (2005) Histone H2AX phosphorylation after cell irradiation with UV-B: relationship to cell cycle phase and induction of apoptosis. *Cell Cycle* **4**: 339–345
- Hoeijmakers JH (2001) Genome maintenance mechanisms for preventing cancer. *Nature* **411**: 366–374
- Hwang BJ, Ford JM, Hanawalt PC, Chu G (1999) Expression of the p48 xeroderma pigmentosum gene is p53-dependent and is involved in global genomic repair. *Proc Natl Acad Sci USA* **96**: 424–428
- Iordanov MS, Pribnow D, Magun JL, Dinh TH, Pearson JA, Chen SL, Magun BE (1997) Ribotoxic stress response: activation of the stress-activated protein kinase JNK1 by inhibitors of the peptidyl transferase reaction and by sequence-specific RNA damage to the alpha-sarcin/ricin loop in the 28S rRNA. *Mol Cell Biol* **17**: 3373–3381
- Iordanov MS, Pribnow D, Magun JL, Dinh TH, Pearson JA, Magun BE (1998) Ultraviolet radiation triggers the ribotoxic stress response in mammalian cells. *J Biol Chem* **273**: 15794–15803
- Jans J, Schul W, Sert YG, Rijkse Y, Rebel H, Eker AP, Nakajima S, van Steeg H, de Gruij FR, Yasui A, Hoeijmakers JH, van der Horst GT (2005) Powerful skin cancer protection by a CPD-photolyase transgene. *Curr Biol* **15**: 105–115
- Kaufmann WK, Kies PE (1998) DNA signals for G2 checkpoint response in diploid human fibroblasts. *Mutat Res* **400**: 153–167
- Kurz EU, Lees-Miller SP (2004) DNA damage-induced activation of ATM and ATM-dependent signaling pathways. *DNA Repair (Amst)* **3**: 889–900
- McKay BC, Stubbert LJ, Fowler CC, Smith JM, Cardamore RA, Spronck JC (2004) Regulation of ultraviolet light-induced gene expression by gene size. *Proc Natl Acad Sci USA* **101**: 6582–6586
- Mitchell DL (1988) The relative cytotoxicity of (6-4) photoproducts and cyclobutane dimers in mammalian cells. *Photochem Photobiol* **48**: 51–57
- Nakajima S, Lan L, Kanno S, Takao M, Yamamoto K, Eker AP, Yasui A (2004) UV light-induced DNA damage and tolerance for the survival of nucleotide excision repair-deficient human cells. *J Biol Chem* **279**: 46674–46677
- Ng JM, Vermeulen W, van der Horst GT, Bergink S, Sugawara K, Vrieling H, Hoeijmakers JH (2003) A novel regulation mechanism of DNA repair by damage-induced and RAD23-dependent stabilization of xeroderma pigmentosum group C protein. *Genes Dev* **17**: 1630–1645
- Niedernhofer LJ, Odijk H, Budzowska M, van Drunen E, Maas A, Theil AF, de Wit J, Jaspers NG, Beverloo HB, Hoeijmakers JH, Kanaar R (2004) The structure-specific endonuclease Ercc1-Xpf is required to resolve DNA interstrand cross-link-induced double-strand breaks. *Mol Cell Biol* **24**: 5776–5787
- O'Driscoll M, Ruiz-Perez VL, Woods CG, Jeggo PA, Goodship JA (2003) A splicing mutation affecting expression of ataxia-telangiectasia and Rad3-related protein (ATR) results in Seckel syndrome. *Nat Genet* **33**: 497–501
- Pages V, Fuchs RP (2002) How DNA lesions are turned into mutations within cells? *Oncogene* **21**: 8957–8966
- Rappold I, Iwabuchi K, Date T, Chen J (2001) Tumor suppressor p53 binding protein 1 (53BP1) is involved in DNA damage-signaling pathways. *J Cell Biol* **153**: 613–620
- Rogakou EP, Boon C, Redon C, Bonner WM (1999) Megabase chromatin domains involved in DNA double-strand breaks *in vivo*. *J Cell Biol* **146**: 905–916
- Sage E (1993) Distribution and repair of photolesions in DNA: genetic consequences and the role of sequence context. *Photochem Photobiol* **57**: 163–174
- Schul W, Jans J, Rijkse YM, Klemann KH, Eker AP, de Wit J, Nikaïdo O, Nakajima S, Yasui A, Hoeijmakers JH, van der Horst GT (2002) Enhanced repair of cyclobutane pyrimidine dimers and improved UV resistance in photolyase transgenic mice. *EMBO J* **21**: 4719–4729
- Schultz LB, Chehab NH, Malikzay A, Halazonetis TD (2000) p53 binding protein 1 (53BP1) is an early participant in the cellular response to DNA double-strand breaks. *J Cell Biol* **151**: 1381–1390
- Squires S, Coates JA, Goldberg M, Toji LH, Jackson SP, Clarke DJ, Johnson RT (2004) p53 prevents the accumulation of double-strand DNA breaks at stalled-replication forks induced by UV in human cells. *Cell Cycle* **3**: 1543–1557
- Stayton CL, Dabovic B, Gulisano M, Gecz J, Broccoli V, Giovanazzi S, Bossolasco M, Monaco L, Rastan S, Boncinelli E (1994) Cloning and characterization of a new human Xq13 gene, encoding a putative helicase. *Hum Mol Genet* **3**: 1957–1964
- Tung BS, McGregor WG, Wang YC, Maher VM, McCormick JJ (1996) Comparison of the rate of excision of major UV photoproducts in the strands of the human HPRT gene of normal and xeroderma pigmentosum variant cells. *Mutat Res* **362**: 65–74
- van Veelen LR, Cervelli T, van de Rakt MW, Theil AF, Essers J, Kanaar R (2005) Analysis of ionizing radiation-induced foci of DNA damage repair proteins. *Mutat Res* **574**: 22–33
- Wang H, Lawrence CW, Li GM, Hays JB (1999) Specific binding of human MSH2.MSH6 mismatch-repair protein heterodimers to DNA incorporating thymine- or uracil-containing UV light photoproducts opposite mismatched bases. *J Biol Chem* **274**: 16894–16900
- Ward IM, Minn K, Chen J (2004) UV-induced ataxia-telangiectasia-mutated and Rad3-related (ATR) activation requires replication stress. *J Biol Chem* **279**: 9677–9680
- Yasui A, Eker APM (1998) DNA photolyases. In *DNA Damage and Repair, Vol. 2: DNA Repair in Higher Eukaryotes*, Nickoloff JA, Hoekstra MF (eds) Vol.2, pp 9–32. Totowa, NJ: Humana Press
- Yoon JH, Lee CS, O'Connor TR, Yasui A, Pfeifer GP (2000) The DNA damage spectrum produced by simulated sunlight. *J Mol Biol* **299**: 681–693